

## Article

# Health Burden and Driving Force Changes Due to Exposure to PM<sub>2.5</sub> and O<sub>3</sub> from 2014 to 2060 in a Typical Industrial Province, China

Chuanyong Zhu <sup>1,\*</sup>, Changtong Zhu <sup>1</sup>, Mengyi Qiu <sup>2</sup>, Yichao Gai <sup>1</sup>, Renqiang Li <sup>1</sup>, Ling Li <sup>3</sup>, Chen Wang <sup>1</sup>, Na Yang <sup>1</sup>, Baolin Wang <sup>1</sup>, Lei Sun <sup>1</sup>, Guihuan Yan <sup>3</sup> and Chongqing Xu <sup>3</sup>

<sup>1</sup> College of Environmental Science and Engineering, Qilu University of Technology (Shandong Academy of Sciences), Jinan 250353, China; 10431211231@stu.qlu.edu.cn (Y.G.); 10431211183@stu.qlu.edu.cn (R.L.); wangchen@qlu.edu.cn (C.W.); yangna@qlu.edu.cn (N.Y.); wangbaolin@qlu.edu.cn (B.W.); sunlei@qlu.edu.cn (L.S.)

<sup>2</sup> State Grid of China Technology Collage, State Grid, Jinan 250002, China; qiumengyi@sgtc.sgcc.com.cn

<sup>3</sup> Ecology Institute of Shandong Academy of Science, Qilu University of Technology (Shandong Academy of Sciences), Jinan 250353, China; liling33802400@qlu.edu.cn (L.L.); yanguihuan@qlu.edu.cn (G.Y.); xucq@sderi.cn (C.X.)

\* Correspondence: zchy@qlu.edu.cn

**Abstract:** While air quality in China has improved significantly in recent years, the population is becoming increasingly vulnerable to air pollution due to the aging population. In this study, we assessed premature deaths attributable to long- and short-term exposures to PM<sub>2.5</sub> and O<sub>3</sub>, as well as their driving forces in Shandong from 2014 to 2060 based on county-level near-real-time air pollutant concentration datasets and projected concentrations of PM<sub>2.5</sub> and O<sub>3</sub>. We found that the concentrations of PM<sub>2.5</sub> and O<sub>3</sub> in most districts and counties from Shandong are still higher than the corresponding concentration limit of Grade II. Premature mortality caused by long- and short-term exposures to PM<sub>2.5</sub> decreased by 13,045 and 8092 in 2020 compared with those in 2014, respectively. Furthermore, premature mortality attributable to short-term exposure to O<sub>3</sub> was 36.08% higher than that due to short-term exposure to PM<sub>2.5</sub> in 2020. The results of the driving force analysis indicate that the health benefits brought about by the improvement in air quality have been offset by the changes in population age structure. In the future, the increase in O<sub>3</sub> concentration and population aging are the top two driving forces having adverse effects on the health burden. This study provides support for controlling the health risks of PM<sub>2.5</sub> and O<sub>3</sub> pollution, especially for the development of dual-pollutant concentration targets and synergistic control strategies.

**Keywords:** PM<sub>2.5</sub>; O<sub>3</sub>; health burden; premature mortality; driving force; Shandong



**Citation:** Zhu, C.; Zhu, C.; Qiu, M.; Gai, Y.; Li, R.; Li, L.; Wang, C.; Yang, N.; Wang, B.; Sun, L.; et al. Health Burden and Driving Force Changes Due to Exposure to PM<sub>2.5</sub> and O<sub>3</sub> from 2014 to 2060 in a Typical Industrial Province, China. *Atmosphere* **2023**, *14*, 1672. <https://doi.org/10.3390/atmos14111672>

Academic Editors: Daniele Contini and Francesca Costabile

Received: 27 September 2023  
Revised: 31 October 2023  
Accepted: 8 November 2023  
Published: 10 November 2023



**Copyright:** © 2023 by the authors. Licensee MDPI, Basel, Switzerland. This article is an open access article distributed under the terms and conditions of the Creative Commons Attribution (CC BY) license (<https://creativecommons.org/licenses/by/4.0/>).

## 1. Introduction

Presently, ambient air pollution has been identified as one of the leading risk factors for human health [1]. The risk assessment data from the Global Burden of Disease (GBD) study indicate that there were 6.45 and 0.35 million premature mortalities attributed to PM<sub>2.5</sub> and O<sub>3</sub> pollution worldwide in 2019, respectively. These are mainly because both short- and long-term exposures to air pollutants (PM<sub>2.5</sub> and O<sub>3</sub>) are associated with an increased risk of all-cause mortality, cardiovascular disease, and respiratory disease [2–4]. To improve air quality and protect public health, a series of stringent action plans and emission standards for comprehensive control of air pollution have been issued by the Ministry of Ecology and Environment of the People’s Republic of China (MEEC) since 2013, which have reduced the risk of PM<sub>2.5</sub> exposure significantly [5]. However, due to the continuous increase in O<sub>3</sub> concentrations and the deepening of the aging population degree, the Chinese population is increasingly vulnerable to air pollution [6–8].

Since 2013, some studies have quantified the health impacts of PM<sub>2.5</sub> and O<sub>3</sub> pollution in China. For example, some of these studies have assessed the health losses and abatement potential caused by PM<sub>2.5</sub> pollution in China based on monitoring station data and World Health Organization (WHO) interim targets [9,10]. Nevertheless, it is difficult to accurately evaluate the air pollution exposure level for the population (especially for the rural population) in the above studies due to the limited number of monitoring sites located in rural areas. With the application of remote sensing technology, Zou et al. [11] estimated PM<sub>2.5</sub>-related premature mortality in China by combining a hybrid remote sensing–geostatistics approach and the exposure factor-enhanced IER model. Subsequently, Yin further explored the spatial and temporal variations in PM<sub>2.5</sub>-related premature mortality and its driving forces at the national level from 1990 to 2019 [12]. As the aggravation of O<sub>3</sub> pollution has improved in recent years, the long- and short-term exposures to O<sub>3</sub> and PM<sub>2.5</sub>-related premature deaths in China [13,14], key areas [15], and megacities [16] have been quantified gradually. For instance, 308 thousand and 16 thousand long- and short-term exposure-related deaths were avoided in 2020 due to the air quality improvement compared with those in 2013, respectively [17].

Especially, previous studies are mainly focused on the quantization of long-term exposure to PM<sub>2.5</sub> and O<sub>3</sub>-related deaths, while studies on the health effects of short-term exposure are limited. As a result of the efforts in reducing PM<sub>2.5</sub>-polluted days and the considerable increase in O<sub>3</sub>-polluted days, Liu et al. [18] indicated that deaths attributable to short-term exposure to O<sub>3</sub> in China are greater than those due to PM<sub>2.5</sub> exposure since 2018. Moreover, only a few studies have distinguished the relative contributions of population changes, pollutant concentrations, age structure, and disease mortality to health losses. Furthermore, most studies have focused on the national or regional level. Based on the results of the literature research conducted in this study, there is a lack of relevant research on long- and short-term exposures to PM<sub>2.5</sub> and O<sub>3</sub>-related deaths in typical industrial and manufacturing provinces at the county-level scale.

In 2020, the government of the P.R. of China announced that China will strive to reach peak CO<sub>2</sub> emissions by 2030 and achieve carbon neutrality by 2060. Being the province with the highest carbon emission [19], Shandong has been constantly ranked as the top place in provincial pollutant emissions due to the predominance of energy-intensive industries in its industrial mix [20]. The clean transition in terms of energy mix and industrial structure should be achieved below the low-carbon emission target in Shandong. As a result, the air quality will be improved significantly because of the remarkable emission reduction in CO<sub>2</sub> and co-emitted air pollutants [21,22]. Especially, the study on the health benefits and its driving force changes due to the air quality improvements at the provincial and municipal levels in the future is limited, although it is critical to understand and develop a long-term pathway for provincial air quality improvements.

Based on the county-level exposure concentrations of air pollutants from the China Air Pollution Tracking Exposure Dataset (TAP, <http://tapdata.org.cn/>, last access: 20 September 2023), the risk assessment data from GBD, and the predicted concentrations of PM<sub>2.5</sub> and O<sub>3</sub> under the Chinese Academy of Environmental Planning Carbon and Air Quality Pathways (CAEP-CAPs), the premature mortality data associated with long- and short-term exposures to PM<sub>2.5</sub> and O<sub>3</sub> in Shandong from 2014 to 2060 are estimated. Meanwhile, the relative contributions of four driving forces (population size change, population aging, mortality change, and exposure concentrations of air pollutants) of health burdens caused by PM<sub>2.5</sub> and O<sub>3</sub> exposure are discussed and quantified. The results provide important references for the formulation and implementation of environmental and public health policies in Shandong and other provinces.

## 2. Methodology

### 2.1. Study Area

As a province with an integrated industrial sector system and an extensive economic development model, Shandong is characterized by significant energy consumption and

remarkable carbon discharge. Moreover, Shandong is the province with the second largest population (approximately 101.7 million in 2020) and the third largest GDP (USD 1.047 trillion in 2020) in China. As a result, the health burden and driving force changes due to PM<sub>2.5</sub> and O<sub>3</sub> exposures in the past and future in Shandong is a problem of widespread concern.

In this study, based on the official regional strategic planning announced in Shandong, 16 cities can be divided into three categories: the Western Economic Rising Belt (WERB), the Provincial Capital City Economic Circle (PCCEC), and the Shandong Peninsula Blue Economic Zone (SPBEZ). The administrative region distributions are shown in Figure 1.

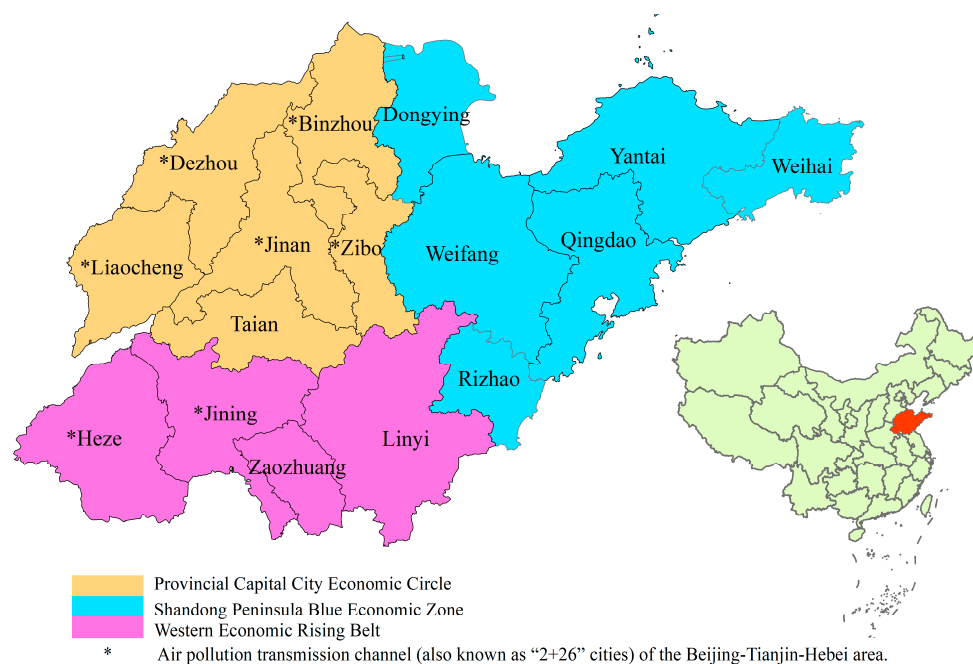


**Figure 1.** Administrative region distributions and city categories of Shandong province.

2.2. Data Sources

The relevant parameters used to evaluate the health burden and driving force contributions caused by PM<sub>2.5</sub> and O<sub>3</sub> exposures and their data sources are shown in Table 1.

**Table 1.** The relevant calculated parameters and their data sources.

Parameters	Data Sources
Daily concentrations of PM <sub>2.5</sub> and O <sub>3</sub> at the county level	Tracking Air Pollution in China ( <a href="http://tapdata.org.cn">http://tapdata.org.cn</a> , last access: 20 September 2023)
Gridded population data (1 km × 1 km)	LandScan Global Population Database ( <a href="https://landscan.ornl.gov/">https://landscan.ornl.gov/</a> , last access: 20 September 2023)
Population proportions in each age group	China Statistical Yearbook ( <a href="http://www.stats.gov.cn/english/">http://www.stats.gov.cn/english/</a> , last access: 20 September 2023)
Baseline mortality of the particular disease categories	China Health Statistical Yearbook ( <a href="http://www.nhc.gov.cn/">http://www.nhc.gov.cn/</a> , last access: 20 September 2023)
Population data for 2025–2060	World Population Prospects 2022 ( <a href="https://population.un.org/wpp/Download/Standard/MostUsed/">https://population.un.org/wpp/Download/Standard/MostUsed/</a> , last access: 20 September 2023)

Specifically, based on the data of the National Population Census and Zhou et al. [23], the annual data of population age structure in Shandong at the district and county level were obtained. Due to the lack of baseline mortality data for diseases at the provincial and municipal levels, statistics on baseline mortality at the national level were used in this study.

### 2.3. Calculated Method

#### 2.3.1. Health Burden Estimation

For the health burden estimation, the integrated exposure–response function (IER) was applied to calculate the relative risk (RR) of specific diseases caused by long-term exposure to PM<sub>2.5</sub>. The relevant calculated equations are listed as follows [24]:

$$RR = 1, \text{ for } C < C_{cf} \tag{1}$$

$$RR = 1 + \alpha \left\{ 1 - \exp \left[ -\gamma (C - C_{cf})^\delta \right] \right\}, \text{ for } C \geq C_{cf} \tag{2}$$

where  $C_{cf}$  is the theoretical minimum-risk concentrations used in the GBD 2019 [1];  $C$  is the annual average PM<sub>2.5</sub> exposure concentration for each district or county;  $\alpha$ ,  $\gamma$ , and  $\delta$  are parameters used to describe the different shapes of the relative risk curves among various diseases, and the relevant values for above parameters are taken from the previously published studies [3,10,14,25]. Especially, there is no additional health risk if the value of  $RR$  for a specific disease is equal to 1.

For long- and short-term exposures to O<sub>3</sub>, as well as for short-term exposure to PM<sub>2.5</sub>, the value of  $RR$  is calculated by using the log-linear exposure–response function [26,27], which is calculated as follows:

$$RR = \exp(\beta(X - X_0)) \tag{3}$$

where  $\beta$  is the exposure–response factor, which refers to the extent of relative risk affected by the concentration changes in PM<sub>2.5</sub> or O<sub>3</sub> [28–30];  $X$  is the exposure concentration of the PM<sub>2.5</sub> or O<sub>3</sub>,  $\mu\text{g}/\text{m}^3$  (the daily average PM<sub>2.5</sub> concentrations and maximum daily 8 h average (MDA8) O<sub>3</sub> concentrations are used to assess the health effects of short-term exposure; the maximum April–September average MDA8 O<sub>3</sub> concentrations are used to assess the health effects of long-term exposure); for long- and short-term exposures to O<sub>3</sub>,  $X_0$  is the WHO background O<sub>3</sub> concentration value ( $70 \mu\text{g}/\text{m}^3$ ); and for short-term exposure to PM<sub>2.5</sub>,  $X_0$  is the WHO guidance value for the air-quality first interim target ( $35 \mu\text{g}/\text{m}^3$ ) [31,32]. Details about the fitted parameters and threshold values used in the exposure–response functions are shown in the Supplementary Materials (SM), Table S1.

The calculated methods of the burden of disease due to long- and short-term exposures to PM<sub>2.5</sub> and O<sub>3</sub> are as follows [29,33,34]:

$$\Delta Mort_{k,j,d} = \sum_{a=25}^{85+} y_{0,k,d,a} \times AF_{k,j,d} \times Pop_{k,j} \times AgeP_{k,j,a} \tag{4}$$

$$AF_{k,j,d} = \frac{RR_{k,j,d} - 1}{RR_{k,j,d}} \tag{5}$$

where  $\Delta Mort_{k,j,d}$  is premature mortality for disease  $d$  (cerebrovascular diseases (CEVDs), International Classification of Diseases Revision 10 codes (ICD-10): I60–I69; ischemic heart diseases (IHDs), ICD-10: I20–I25; lung cancer (LC), ICD-10: C33–C34; chronic obstructive pulmonary diseases (COPDs), ICD-10: J40–J47; cardiovascular diseases (CVDs), ICD-10: I00–I99; and respiratory disease (RD), ICD-10: J00–J99) in the district (or county)  $j$  at the year of  $k$ ;  $y_{0,k,d,a}$  is the baseline mortality rate (see SM, Table S2) for disease  $d$  at the age group  $a$  (25–29, 30–34, 35–39, 40–44, 45–49, 50–54, 55–59, 60–64, 65–69, 70–74, 75–79, 80–84, and  $\geq 85$ ) in year  $k$ . For the baseline mortality rates from 2025 to 2060, the relevant values are assumed to be constant in the different scenarios, consistent with the 2020 level.  $RR_{k,j,d}$  is the relative risk of disease  $d$  in district  $j$  in year  $k$ ;  $Pop_{k,j}$  is the number of people in district  $j$  in year  $k$ .  $AgeP_{k,j,a}$  is the proportion of the population in age group  $a$  in  $j$  district in  $k$  year.  $AF_{k,j,d}$  is the attributable fractions (AFs) of  $d$  disease in district  $j$  in year  $k$ .

### 2.3.2. Analysis of Driving Forces

There are four factors, including population growth, population aging, mortality rates independent of exposure to air pollutants, and exposure concentration of air pollutants, that contribute to total mortality attributable to air pollution, and changes in these factors bring about the overall change in attributable mortality [35]. The decomposition method from Cohen et al. [35] was adopted to quantify the respective driving force of premature mortality for population size change, population aging, mortality rate change, and pollutant (PM<sub>2.5</sub> or O<sub>3</sub>) exposure concentration change. Summarily, the change in one factor was allowed during the driving force analysis from the start year to the target year while other factors remained consistent with those at the start year (only one factor changes at each cycle). Eventually, population growth effect ( $H_{pop}$ ), population aging effect ( $H_{age}$ ), baseline mortality rate change effect ( $H_{base}$ ), and exposure change effect ( $H_{exposure}$ ) were calculated. The corresponding driving forces of premature mortality were calculated as follows:

$$\Delta Mort_{k,j,d} = \sum_{a=25}^{85+} y_{0,s,d,a} \times AF_{s,j,d} \times Pop_{s,j} \times AgeP_{s,a} \quad (6)$$

$$A_t = \sum_{a=25}^{85+} y_{0,s,d,a} \times AF_{s,j,d} \times Pop_{t,j} \times AgeP_{s,a} \quad (7)$$

$$B_t = \sum_{a=25}^{85+} y_{0,s,d,a} \times AF_{s,j,d} \times Pop_{t,j} \times AgeP_{t,a} \quad (8)$$

$$C_t = \sum_{a=25}^{85+} y_{0,t,d,a} \times \left( \frac{1 - AF_{t,j,d}}{1 - AF_{s,j,d}} \right) \times AF_{s,j,d} \times Pop_{t,j} \times AgeP_{t,a} \quad (9)$$

$$\Delta Mort_{t,j,d} = \sum_{a=25}^{85+} y_{0,t,d,a} \times AF_{t,j,d} \times Pop_{t,j} \times AgeP_{t,a} \quad (10)$$

$$H_{pop} = A_t - \Delta Mort_{s,j,d} \quad (11)$$

$$H_{age} = B_t - A_t \quad (12)$$

$$H_{base} = C_t - B_t \quad (13)$$

$$H_{exposure} = \Delta Mort_{t,j,d} - C_t \quad (14)$$

where  $A_t$ ,  $B_t$ , and  $C_t$  are intermediate variables [5,12,36];  $s$  is the start year;  $t$  is the target year;  $H_{pop}$  represents the population growth effect;  $H_{age}$  represents the population aging effect;  $H_{base}$  represents the baseline mortality rate change effect; and  $H_{exposure}$  represents the exposure change effect. The meanings of other parameters are consistent with the previous text.

The sequence of adding factors also influences the results when using this method of sensitivity analysis. We calculated the results for all 24 sequences of the four factors, and the final estimation of the contributions of the different factors is the average value of the results for each factor.

## 3. Results and Discussion

### 3.1. Spatial–Temporal Variation Characteristics of PM<sub>2.5</sub> and O<sub>3</sub> Concentrations

In general, the air quality of Shandong has been improved significantly with the implementation of a series of clean air actions such as the Air Pollution Prevention and Control Action Plan (APPCAP) and the Blue Sky Defense Action (BSDA) from 2013 to 2020 (for more details, see SM, Table S4). The spatial and temporal distributions of annual average concentrations of PM<sub>2.5</sub> and the annual April–September average concentration

of MDA8 O<sub>3</sub> in Shandong from 2014 to 2020 are shown in Figure 2. As can be seen, for MDA8 O<sub>3</sub>, the annual April–September average concentrations in Shandong increased from 116.8 µg/m<sup>3</sup> in 2014 to 139.2 µg/m<sup>3</sup> in 2020, with an annual growth rate of 2.97%. Especially, the 90th percentile of the April–September average concentration of MDA8 O<sub>3</sub> in Shandong in 2020 was 7.14% higher than the concentration limit of Grade II (160 µg/m<sup>3</sup>) issued by the China Ambient Air Quality Standards (CAAQS) (GB3095-2012). During the same period, the annual average concentrations of PM<sub>2.5</sub> exhibited a significant decrease from 79.5 µg/m<sup>3</sup> to 44.8 µg/m<sup>3</sup>. However, the annual average concentrations of PM<sub>2.5</sub> in most districts and counties from Shandong are still higher than the annual average concentration limit of Grade II (35 µg/m<sup>3</sup>).

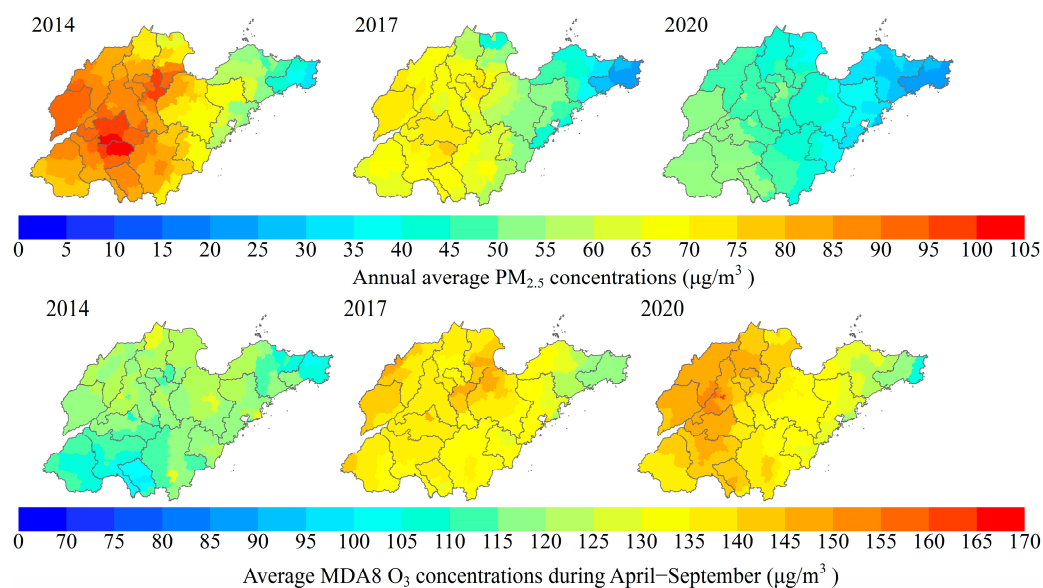


**Figure 2.** The distributions of annual average concentrations of PM<sub>2.5</sub> and annual April–September average concentrations of MDA8 O<sub>3</sub> in Shandong, 2014–2020.

In order to further analyze the temporal distribution characteristics of primary pollutants, the monthly variation characteristics of MDA8 O<sub>3</sub> and PM<sub>2.5</sub> concentrations in Shandong from 2014 to 2020 are displayed in Figure 3. As can be seen, the monthly variation trends of PM<sub>2.5</sub> concentrations exhibit the u-shaped distribution feature throughout the year, with the highest concentration in winter. These are mainly because the stable vertical structure of the atmosphere in winter hinders the vertical diffusion and dilution of air pollutants. As a result, meteorological conditions suitable for pollutant accumulation are formed especially in low wind speed areas [37–39]. Meanwhile, the emissions of particulate matter from anthropogenic sources are higher in the heating season than those in the non-heating season due to the remarkable coal consumption [40,41]. Specifically, the coal consumption used for heat supply is estimated at about 82.44 Mt, accounting for about 21.14% of the provincial total coal consumption [42]. In contrast, the monthly average concentrations of MDA8 O<sub>3</sub> exhibit n-shaped distribution characteristics, with the highest concentration in summer. The comprehensive interactions between meteorological factors (e.g., high temperature and strong solar radiation) and precursor pollutant (e.g., NO<sub>x</sub> and VOCs) emissions may be responsible for the significant seasonal and spatial variability in O<sub>3</sub> pollution in Shandong [43]. Dang et al. [44] found that the increase of 2 m temperature and the anomaly of meridional wind at 850 hPa are regarded as the two main meteorological driving forces for O<sub>3</sub> concentration enhancement in the North China Plain. As a typical VOC-limited area, the increase in VOC emissions or the non-synergistic reduction in NO<sub>x</sub> and VOC emissions will lead to an increase in O<sub>3</sub> concentration in Shandong [45].

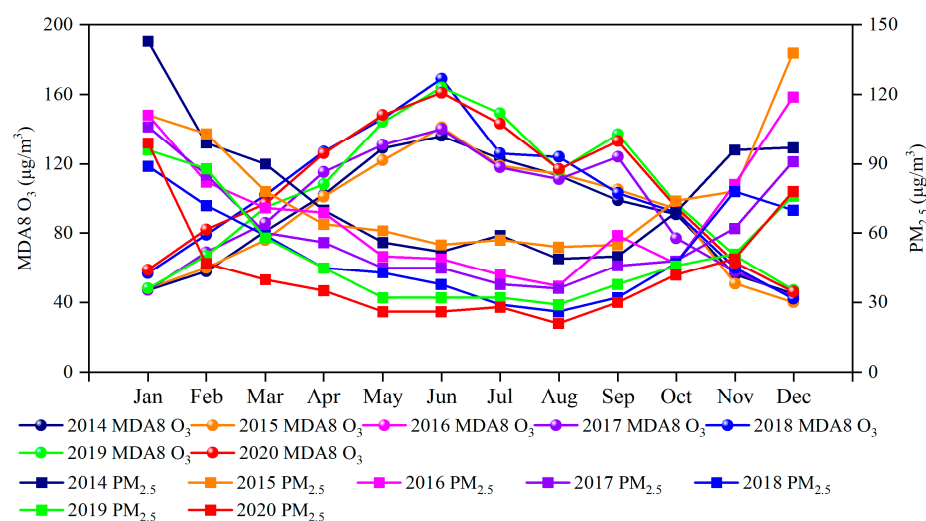


**Figure 3.** Monthly average concentration variations in MDA8 O<sub>3</sub> and PM<sub>2.5</sub> in Shandong, 2014 to 2020.

In this study, the variation trends of the annual April–September average MDA8 O<sub>3</sub> concentrations and annual average PM<sub>2.5</sub> concentrations for each county in PCCEC, WERB, and SPBEZ from 2014 to 2020 were further analyzed (see SM, Figure S1). As can be seen, the 7-year annual average PM<sub>2.5</sub> concentrations in WERB and PCCEC are 39.42% and 43.19% higher than those in the SPBEZ, respectively. This is mainly because the eastern peninsula region is easily influenced by the sea–land circulation process, which can bring about the rapid spreading of atmospheric particles [46]. Especially, with the implementation of the working scheme of air pollution control for Beijing–Tianjin–Hebei and surrounding regions in 2017, the annual average PM<sub>2.5</sub> concentrations decreased significantly in air pollution transmission channel cities (see Figures 1 and 2). Specifically, the annual average decrease rates of PM<sub>2.5</sub> concentrations in PCCEC are the highest (about 10.78%) among the three areas from 2017 to 2020.

Unlike the decline in annual average PM<sub>2.5</sub> concentrations, the increments of annual April–September average MDA8 O<sub>3</sub> concentrations in WERB and PCCEC are 163.64% and 145.46% greater than those in SPBEZ from 2014 to 2020. There is an inverse correlation between the annual April–September average MDA8 O<sub>3</sub> concentrations and annual average PM<sub>2.5</sub> concentrations. This correlation is mainly because of the depression of the heterogeneous absorption of HO<sub>2</sub> by aerosol with the decline in PM<sub>2.5</sub> concentrations [7,47].

Meanwhile, we also observed differences in PM<sub>2.5</sub> and O<sub>3</sub> concentrations in Shandong during the pre- to post-lockdown periods of COVID-19 (SM, Figure S2a,b). The PM<sub>2.5</sub> concentration in Shandong during the COVID-19 lockdown period and the post-lockdown period in 2020 decreased by 28.68 µg/m<sup>3</sup> (33%) and 18.14 µg/m<sup>3</sup> (30%) compared with those during the same period in 2019, respectively. In contrast to PM<sub>2.5</sub>, we observed a different pattern of changes in O<sub>3</sub> concentrations. Compared with O<sub>3</sub> concentrations during the same period in 2019, the average concentration of O<sub>3</sub> increased by 7.11 µg/m<sup>3</sup> (9%) during the lockdown period, while the average concentration of O<sub>3</sub> decreased by 6.4 µg/m<sup>3</sup> (6%) during the post-lockdown period. These changes are mainly attributed to the restrictions on transportation, the decrease in industrial activities, and the imbalance of the emission reductions in O<sub>3</sub> precursors. People realized that reducing travel and contact with others effectively reduced the spread of the virus. Thus, the decreasing trend of O<sub>3</sub> concentration remained unchanged after the end of the COVID-19 lockdown. These findings provide important insights for assessing the effectiveness of the implementation of environmental control measures.

In a word, as the important precursors for the generation of secondary PM<sub>2.5</sub> and O<sub>3</sub>, reasonable reductions in VOCs and NO<sub>x</sub> emissions can help to achieve the synergetic control of PM<sub>2.5</sub> and O<sub>3</sub> pollution and improve air quality continuously.

### 3.2. Health Burdens of Long- and Short-Term Exposures to PM<sub>2.5</sub> and O<sub>3</sub>

#### 3.2.1. Health Burden of Long-Term Exposure to PM<sub>2.5</sub> and O<sub>3</sub>

The health endpoints and premature mortality associated with long-term exposure to PM<sub>2.5</sub> and O<sub>3</sub> in Shandong from 2014 to 2020 are listed in Figure 4a,b. As can be seen, the premature mortality associated with long-term exposure to PM<sub>2.5</sub> was the highest in 2015 (about  $1.2 \times 10^5$ ). This is mainly because the number of people exposed to high PM<sub>2.5</sub> concentrations in 2015 is higher than those in subsequent years (see SM, Figure S3). Although the cumulative distribution trends of the resident population under different ambient PM<sub>2.5</sub> concentrations in Shandong are overall consistent between 2014 and 2015, the baseline mortality for IHD in the age group 50–54 (male) in 2015 is 12.43% higher than that in 2014 (more details about baseline mortality for specific diseases from 2014 to 2020 can be seen in SM, Table S2). Subsequently, an overall downward trend was found, from  $1.2 \times 10^5$  (178.6 per 100,000) in 2015 to  $1.0 \times 10^5$  (145.2 per 100,000) in 2020. Furthermore, the proportions of premature mortality associated with long-term PM<sub>2.5</sub> exposure relative to provincial total deaths decreased from 18.7% in 2015 to 15.5% in 2020, indicating that public health has improved to some extent with the implementation of strict air pollution control measures.

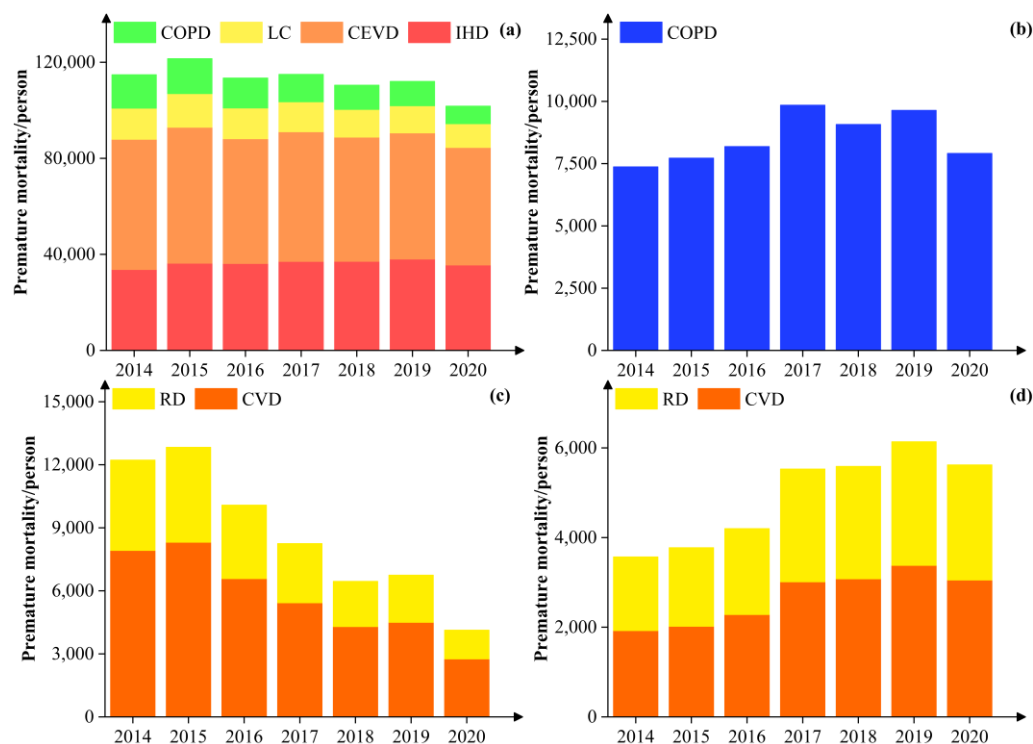


**Figure 4.** Premature mortality due to long-term exposure to PM<sub>2.5</sub> (a) and O<sub>3</sub> (b) and short-term exposure to PM<sub>2.5</sub> (c) and O<sub>3</sub> (d) in Shandong, 2014–2020.

The spatial distribution characteristics of premature mortality caused by long-term exposures to PM<sub>2.5</sub> and O<sub>3</sub> in Shandong at the county level from 2014 to 2020 are displayed in Figure 5a,b. As shown in the figure, premature mortality varies significantly among counties. Among them, Pingdu district of Qingdao (1750), Tengzhou district of Zaozhuang (1710), Xintai county of Tai'an (1423), Caoxian county of Heze (1416), Lanling county of Linyi (1283), Laizhou district of Yantai (1275), Danxian county of Heze (1274), Shouguang district of Weifang (1270), Mudan district of Heze (1256), and Shibeidistrict of Qingdao (1233) are the top 10 counties with the highest premature mortality rates in 2020, accounting for about 13.65% of the provincial total premature mortality (see SM, Table S5 for more details). From the perspective of cities, the highest premature mortality rates due to long-term exposure to PM<sub>2.5</sub> were found in Linyi, Weifang, and Qingdao. As mentioned

above, premature mortality has decreased remarkably with the improvement in air quality. Specifically, the annual average decrease rates of premature mortality caused by long-term exposure to PM<sub>2.5</sub> at the city level from 2014 to 2017 and 2017 to 2020 are estimated at about  $-4.68\sim-0.85\%$  and  $-5.24\sim-1.64\%$ , respectively (SM, Figure S4a). Although air pollution prevention actions have been implemented for several years, premature mortality associated with long-term exposure to PM<sub>2.5</sub> is still at a high level. In terms of contribution proportions of premature mortality for diseases, the share of premature mortality for IHD caused by long-term exposure to PM<sub>2.5</sub> presents an increasing trend from 29.3% in 2014 to 34.9% in 2020. However, the contribution proportions of premature mortality for COPD and LC caused by long-term exposure to PM<sub>2.5</sub> show opposite variation trends during the same period. These are mainly determined by the sensitivity differences of the relative risk of each disease for the variation in PM<sub>2.5</sub> concentration, the interannual changes in the exposure population, and the baseline mortality, etc. Especially, IHD and CEVD are the primary diseases having an adverse effect on the public health burden, accounting for over 79% of the PM<sub>2.5</sub>-attributable mortality. By 2020, the interannual contribution proportions of CEVD, IHD, LC, and COPD were 48.1%, 34.9%, 9.7%, and 7.2%, respectively (see SM, Table S6).

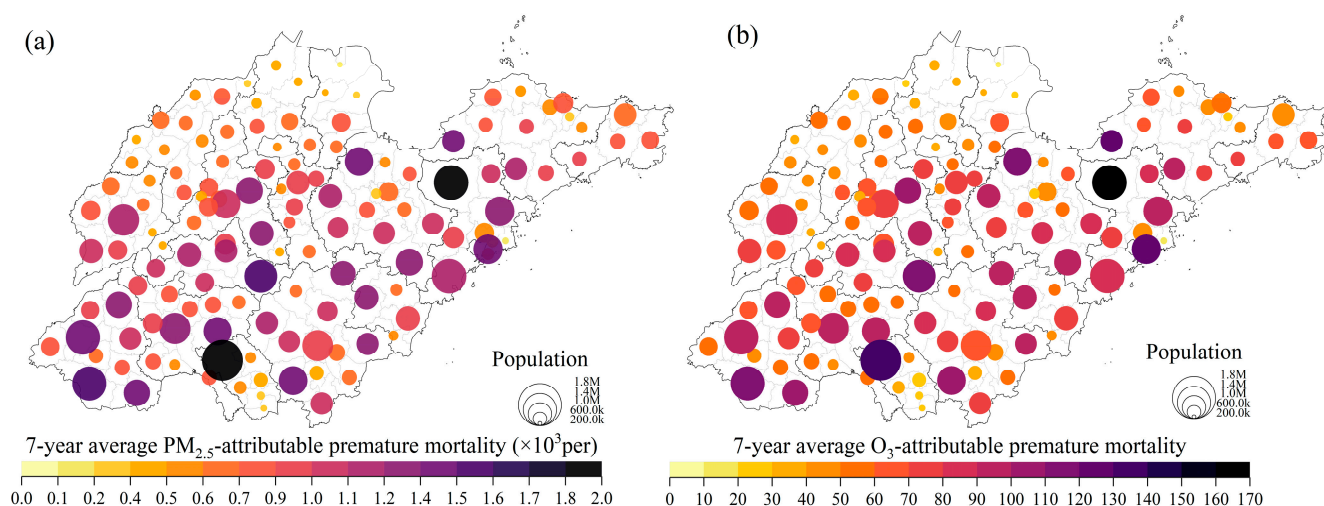


**Figure 5.** Spatial distribution of premature mortality due to long-term exposure to PM<sub>2.5</sub> (a) and O<sub>3</sub> (b) in Shandong at the county level, 2014–2020.

According to the set of AF change curves for each health endpoint at the corresponding PM<sub>2.5</sub> concentrations (see SM, Figure S5), we found the dynamic response of the AFs of CEVD and IHD to be significant at low PM<sub>2.5</sub> concentrations. These results are mainly because the exposure–response curve is non-linear, with a more significant rate of change in the slope at low concentration ranges [3]. Therefore, it is more beneficial for the decrease in the AFs of CEVD and IHD to further reduce the PM<sub>2.5</sub> concentration in the future. Furthermore, the response of the AFs of CEVD for PM<sub>2.5</sub> concentrations is much more sensitive than that of IHD. For example, the PM<sub>2.5</sub> concentrations in the Rongcheng district of Weihai and Sishui county of Jining decreased by about 37.1% (from 35  $\mu\text{g}/\text{m}^3$  to 22  $\mu\text{g}/\text{m}^3$ ) and 53.4% (from 103  $\mu\text{g}/\text{m}^3$  to 48  $\mu\text{g}/\text{m}^3$ ) from 2014 to 2020, respectively. Correspondingly, the AFs of CEVD in the Rongcheng district of Weihai and Sishui county of Jining were reduced by about 11.3% and 7.6%, respectively, while the AFs of IHD in both counties only reduced by about 5.5% and 6.2%, respectively.

The results of source apportionment show that secondary aerosol generation is the major emission source of PM<sub>2.5</sub> in Central and Eastern China [48–50]. Cheng et al. [51] indicate that the more serious the pollution is, the higher the proportion of secondary particle generation is (from 20% to 41%). This implies that the targeted policies and

measures for reducing secondary aerosol generation should be issued and implemented to achieve excellent health benefits in the future.

In general, premature mortality for COPD caused by long-term exposure to O<sub>3</sub> presents a trend of increasing first and decreasing thereafter from 2014 to 2020 (Figure 4b). The highest value occurred in 2017 (about 9849). By 2020, the data discussed above decreased by 19.67% compared with that in 2017. In addition, there is significant heterogeneity in premature mortality data caused by long-term exposure to O<sub>3</sub> in different counties from 16 cities (Figure 5b). Among the top 30 counties with the highest premature mortality due to long-term exposure to O<sub>3</sub> from 2014 to 2020, the total number of premature deaths is estimated at approximately 21,091, accounting for about 30.9% of the provincial total of premature mortality attributed to long-term exposure to O<sub>3</sub> (see SM, Table S7 for more details). The counties with high premature mortality are often characterized by high population density. Jiang et al. [52] and Zhou et al. [53] indicate that the emissions of NO<sub>x</sub> and VOCs from motor vehicles, solvent use, and industrial processes are remarkable in densely urban areas. As a result, the health burdens attributed to the elevation in O<sub>3</sub> concentration increase significantly, especially in urban areas. Linyi, Weifang, Qingdao, Jinan, Heze, and Jining are the top six cities with the highest premature mortality due to long-term O<sub>3</sub> exposure from 2014 to 2020, contributing to about 10.2%, 10.1%, 8.7%, 8.4%, 8.3%, and 8.1% of the provincial total of premature mortality, respectively (SM, Figure S4b).

As discussed above, the formation mechanism of O<sub>3</sub> is complex and is influenced by multiple factors. There are rare studies about this aspect at present in 16 cities of Shandong. Zhu et al. [54] indicate that the concentration of O<sub>3</sub> increased significantly in the North China Plain and Yangtze River Delta during the COVID-19 lockdown period due to the enhancement of atmospheric oxidation capacity associated with the meteorology and emission reduction. Therefore, O<sub>3</sub> control policies should ensure reasonable emission reductions in VOCs and NO<sub>x</sub> to maintain stable O<sub>3</sub> formation regimes and atmospheric oxidation capacity levels and thereby decrease the health burdens associated with O<sub>3</sub> pollution.

### 3.2.2. Health Burden of Short-Term Exposure to PM<sub>2.5</sub> and O<sub>3</sub>

The health endpoints and premature mortality associated with short-term exposures to PM<sub>2.5</sub> and O<sub>3</sub> in Shandong from 2014 to 2020 are listed in Figure 4c,d. As can be seen, premature mortality associated with short-term exposures to PM<sub>2.5</sub> decreased from 12,222 (95% CI: 6553~17,615) in 2014 to 4130 (95% CI: 2136~6147) in 2020, with an annual average decrease rate of 16.5%. Therein, the annual average decrease rate in SPBEZ is estimated at about 17.86%, which is 0.96% and 2.64% higher than those in PCCEC and WERB, respectively (see SM, Figure S6). Furthermore, premature mortality attributed to short-term exposure to PM<sub>2.5</sub> in 16 cities at different pollution levels is discussed in this study. Specifically, the shares of premature mortality caused by light, moderate, heavy, and serious pollution were 35.8%, 33.1%, 19.6%, and 11.5% in 2020, respectively. Premature mortality caused by short-term exposure to PM<sub>2.5</sub> in Linyi was the highest, followed by Jining and Heze (see SM, Figure S7). These results are mainly due to Linyi having the largest population base (11.03 million) and high PM<sub>2.5</sub> pollution levels.

Premature mortality caused by short-term exposure to PM<sub>2.5</sub> increased by about 4.6% in 2019 compared with 2018. This result is mainly because the unfavorable meteorological diffusion conditions and the slowdown of pollutant reduction combine to bring about the re-increase in PM<sub>2.5</sub> concentration [55]. In particular, unfavorable meteorological conditions in the fall and winter can play a greater role in controlling heavy pollution episodes [56], which tends to exacerbate the health burden of short-term exposures. For instance, meteorological conditions are regarded as one of the main contributors to the decrease in PM<sub>2.5</sub> concentration from 2015 to 2019, with a reduction of 15.7~18.6%. However, the meteorological conditions in 2019 were less conducive to pollutant diffusion than those in previous years [39]. It is significant to assess the health effects of short-term exposure to air pollutants during the COVID-19 pandemic. We find that premature deaths due to short-term exposure to PM<sub>2.5</sub> during the COVID-19 lockdown period decreased by 907

(95% CI: 501–1299) compared with that during the same period in 2019 (SM, Figure S2c), which is attributed to the reduction in anthropogenic emissions. Therefore, to achieve the maximum health benefits, both meteorological diffusion and emission effects for air pollutants should be considered when developing and implementing control strategies.

CVD is more easily affected by short-term  $PM_{2.5}$  exposure than RD. Concretely, premature mortality attributed to CVD is about 5683 (seven-year average), which is twice the premature mortality attributed to RD (see SM, Table S6). This result is mainly attributed to population aging [57]. Wang et al. [58] indicate that short-term exposure to  $PM_{2.5}$  can alter cardiac autonomic function and increase the risk of cardiovascular events in the elderly. Therefore, healthcare services for the elderly population should be enhanced to reduce the health burden of ambient air pollution [59].

Unlike  $PM_{2.5}$ , although premature mortality associated with short-term exposure to  $O_3$  in Shandong fluctuates in certain years, the increasing trend can be found from 2014 to 2020 in general (see Figure 4d). Specifically, premature mortality associated with short-term  $O_3$  exposure increased from 3570 (95% CI: 473–6544) in 2014 to 5622 (95% CI: 1008–10,156) in 2020, with an annual growth rate of 7.9%. The seven-year average number of premature mortality caused by short-term exposure to  $O_3$  is higher in Qingdao (502), Dezhou (502), and Jining (440) among 16 cities in Shandong (see SM, Table S8). Premature mortality in Zaozhuang (103) was the lowest because of the small population scale. It is noteworthy that premature mortality dropped in almost 16 cities in 2020. This result is mainly due to the reduction in the number of polluted days with  $O_3$  as the primary pollutant. Premature deaths due to short-term exposure to  $O_3$  increased by 63 (95% CI: 14–110) during the COVID-19 lockdown period in 2020 compared with that during the same period in 2019. However, premature deaths decreased by 128 (95% CI: 30–225) during the post-lockdown period in 2020 (SM, Figure S2d). Zheng et al. [60] confirm that most of the pandemic-related emission reductions occurred before April 2020, so the favorable meteorological diffusion conditions may be the main reason for bringing about the above phenomenon.

In 2020,  $O_3$  is regarded to be the dominant pollutant in the contribution of short-term health effects. Premature mortality associated with short-term exposure to  $O_3$  is 36.08% higher than that caused by short-term exposure to  $PM_{2.5}$ . Therefore, the synergistic control of  $PM_{2.5}$  and  $O_3$  should be emphasized in short-term emergency plans and long-term air pollution control strategies in the future.

### 3.3. Driving Forces of Health Burden

In this study, four driving forces having an impact on the premature mortality associated with long-term exposure to  $PM_{2.5}$  and  $O_3$  are discussed, including  $H_{pop}$ ,  $H_{age}$ ,  $H_{base}$ , and  $H_{exposuer}$ . As shown in Figure 6, premature mortality decreased by 33,858 (95% CI: 18,098–39,608) and 5947 (95% CI: 4913–6272) in 2020 due to the variations in  $H_{exposuer}$  ( $PM_{2.5}$ ) and  $H_{base}$  compared with those in 2014, respectively. Nevertheless, the changes in  $H_{pop}$  and  $H_{age}$  brought about an increase in premature mortality of 3265 (95% CI: 1455–4592) and 23,495 (95% CI: 12,247–31,428) in 2020 compared with those in 2014, respectively.

Population aging is the main driving force of the increase in premature mortality. Concretely, premature mortality caused by population aging increased by 7514 (95% CI: 5156–10,444), 10,564 (95% CI: 4509–13,604), 2693 (95% CI: 1065–3617), and 2724 (95% CI: 1517–3762) for IHD, CEVD, LC, and COPD in 2020, accounting for 22.3%, 19.5%, 20.7%, and 19.5% of the corresponding total changes in premature mortality for each health endpoint compared with those in 2014, respectively (see SM, Table S9).

In order to further analyze the adverse effects on health endpoint caused by population aging, the percentages of premature mortality for IHD and CEVD associated with long-term exposure to  $PM_{2.5}$  based on sex and age groups in Shandong from 2014 to 2020 are discussed (see Figure 7). As can be seen, the proportions (number) of premature deaths associated with IHD and CEVD for the male population aged 85+ increased from 15.7% (2701) and 11.7% (3458) in 2014 to 19.9% (3606) and 15.3% (4097) in 2020. For the female population aged 85+, the above relevant values are much higher than those for males



from 2014 to 2017. There is a significant adverse effect on health burden by the increase in O<sub>3</sub> concentration bringing about the increases of 2982 (95% CI: 1554~4736) and 261 (95% CI: 137~393) in O<sub>3</sub>-attributable premature mortality, accounting for 40.5% and 2.7% of the variations in premature mortality from 2014 to 2017 and 2017 to 2020, respectively. These are mainly because the annual average growth rate of April–September MDA-8 h O<sub>3</sub> concentrations from 2014 to 2017 is 6.7 times higher than that from 2017 to 2020. From 2017 to 2020, population aging is thought to be the main driving force of the increase in health burden associated with long-term exposure to O<sub>3</sub>, which contributes to an increase of 985 (95% CI: 600~1431) in O<sub>3</sub>-attributable premature mortality. The health benefits of improved COPD-related healthcare are observed within both periods, which leads to a decrease of 1435 (95% CI: 711~2564) and 3223 (95% CI: 1761~4918) in premature mortality associated with long-term exposure to O<sub>3</sub> in Shandong from 2014 to 2017 and 2017 to 2020, respectively.

It is worth noting that the problem of population aging is inevitable compared with other factors. The adverse impacts on health burden will be reinforced with the rise in O<sub>3</sub> concentrations and the aggravation of population aging. Therefore, work focused on decreasing O<sub>3</sub> concentrations and improving medical conditions should be emphasized to reduce premature mortality caused by long-term exposure to O<sub>3</sub> in the future.

### 3.4. Assessment of Health Burden and Its Driving Forces under the CAEP-CAP Pathway from 2020 to 2060

Premature mortality and the changes in driving forces caused by long-term exposure to PM<sub>2.5</sub> and O<sub>3</sub> under the CAEP-CAP pathway in Shandong from 2020 to 2060 are illustrated in Figure 8. With the implementation of low-carbon policies and the issue of stricter emission standards in the future, the significant decrease in PM<sub>2.5</sub> and O<sub>3</sub> concentrations is bringing about huge health benefits in Shandong, beginning in 2020 and into the future up to 2060. Specifically, the number of PM<sub>2.5</sub>-related premature deaths caused by the reduction in PM<sub>2.5</sub> concentration will decrease by 46,772 in 2035 compared with that in 2020. Nevertheless, the above-related value of premature mortality in 2060 is 128,812 lower than that in 2035. Shi et al. [62] indicate that the emission reductions in air pollutants are still mainly dependent on process management and the widespread application of advanced end-of-pipe control devices before 2035. It implies that the health benefits attributed to the decrease in PM<sub>2.5</sub> concentration can be fulfilled by the innovation of emission control technology and the rigorous management of industrial processes. The low-carbon policies characterized by the curtailment of fossil energy consumption will play a significant role in the reduction in air pollutant emissions and the increase in health benefits from 2035 to 2060.

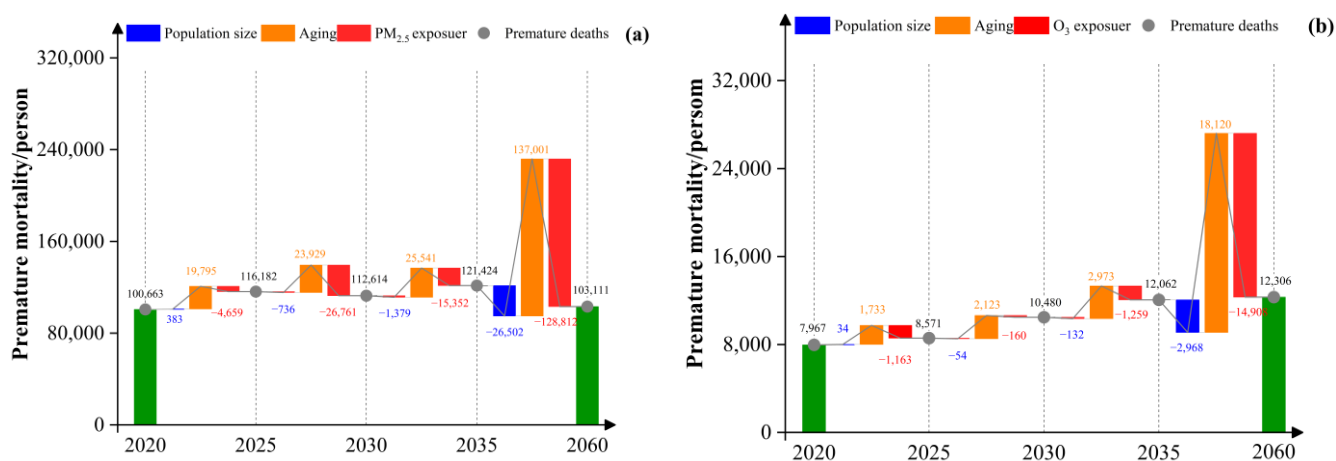


Figure 8. Premature mortality and driving force changes in long-term PM<sub>2.5</sub> (a) and O<sub>3</sub> (b) exposure under the CAEP-CAP pathway in Shandong, 2020–2060.

Generally, the variation trends of premature mortality caused by the decrease in  $O_3$  concentrations from 2020 to 2060 are consistent with the variation trends of premature mortality caused by the decrease in  $PM_{2.5}$  concentrations. However, the positive effects on premature mortality attributed to the decrease in  $O_3$  concentration are much lower than those of  $PM_{2.5}$ . Specifically, the total premature mortality arising from the decrease in  $PM_{2.5}$  and  $O_3$  concentrations are estimated at about 175,584 and 17,490 from 2020 to 2060, respectively. This is mainly because precursor emissions may impact  $O_3$  concentrations in non-linear and interdependent manners [63]. Previous studies have shown that limited  $NO_x$  emission control without regional involvement in short periods may enhance the risk of increasing urban  $O_3$  pollution levels due to the VOC-limited conditions [64]. In addition, Shandong is the province with the highest industrial VOC emissions in China, of which tire manufacturing, the pharmaceutical sector, oil refining, and the coal coking industry are the main anthropogenic emission sources, accounting for approximately more than 50% of the provincial total VOC emissions [65]. However, there are still many problems in controlling VOC emissions in the above sectors, such as the low removal efficiencies of end-of-pipe treatment measures, the limitation of refined control ability, and the huge unorganized emission of VOCs. Thus, reducing ground-level  $O_3$  concentrations poses a particularly difficult challenge for air pollution control in Shandong.

On the other hand, although the vulnerability of the population increases continuously with the increasing proportion of the elderly in the population (see SM, Figure S8), the increase in premature mortality caused by long-term exposure to  $PM_{2.5}$  and  $O_3$  is shown to be suppressed from 2020 to 2060 in Figure 8. These are the combined results of a competitive selection between the high vulnerability of the elderly population to  $PM_{2.5}$  and  $O_3$  pollution due to the increasing aging population and the decrease in  $PM_{2.5}$  and  $O_3$  concentrations caused by the application of advanced air pollutant control devices (APCDs) and the implementation of low-carbon policies. Specifically, the number of  $PM_{2.5}$ -related and  $O_3$ -related premature mortalities arising from population vulnerability increased remarkably by 206,266 and 24,949 in 2060 compared with those in 2020, respectively. Especially, the positive effects on premature mortality attributable to the decrease in  $PM_{2.5}$  and  $O_3$  concentrations cannot be counteracted completely by the adverse effects on health benefits of population aging, which is consistent with the results from Geng et al. [5].

#### 4. Conclusions

Based on the real-time exposure concentrations of air pollutants at the county level, the risk assessment data, and the predicted concentrations of  $PM_{2.5}$  and  $O_3$ , the health burden and driving force changes due to exposure to  $PM_{2.5}$  and  $O_3$  in Shandong from 2014 to 2060 were quantified. We found that the accumulation amount of premature mortality associated with long- and short-term exposures to  $PM_{2.5}$  and  $O_3$  is estimated at about 848,797 and 95,141 from 2014 to 2020. Therein, IHD and CEVD are the primary diseases having an adverse effect on the public health burden, accounting for over 79% of the  $PM_{2.5}$ -attributable mortality. For the spatial distribution characteristics of premature mortality at the county level, Pingdu district of Qingdao (1890), Tengzhou district of Zaozhuang (1847), Xintai county of Taian (1531), Caoxian county of Heze (1521), and Lanling county of Linyi (1384) are the top five counties with the highest premature mortality in 2020. Especially,  $O_3$  was identified as the dominant pollutant in the contribution of short-term health effects in 2020. Furthermore, as the aggravation of population aging increases, the vulnerability of the population due to exposure to air pollutants is further enhanced. However, the adverse effects on health benefits attributed to the population aging can be suppressed in the future. These are the combined results of a competitive selection between the high vulnerability of the elderly population at high exposure levels of air pollutants due to the increasing aging population and the decrease in  $PM_{2.5}$  and  $O_3$  concentrations caused by the application of APCDs and the implementation of low-carbon policies. Furthermore, the positive effects on premature mortality attributed to the decrease in  $O_3$  concentration are much lower than those of  $PM_{2.5}$  in the future. As the province with the highest industrial VOC emissions in

China, reducing ground-level O<sub>3</sub> concentrations poses a particularly difficult challenge for air pollution control in Shandong. In conclusion, the cooperative control of PM<sub>2.5</sub> and O<sub>3</sub> pollution and the implementation of low-carbon policies can be considered as a long-term mechanism to improve health benefits in the future.

**Supplementary Materials:** The following supporting information can be downloaded at: <https://www.mdpi.com/article/10.3390/atmos14111672/s1>. Figure S1. Annual April–September average MDA8 O<sub>3</sub> concentrations and annual average PM<sub>2.5</sub> concentrations for each district and county in PCCEC, WERB, and SPBEZ from 2014 to 2020. Figure S2. Comparative analysis of PM<sub>2.5</sub> (a) and O<sub>3</sub> (b) concentration variations in Shandong province during the Pre-lockdown (6 January–22 January), Lockdown (23 January–28 February), and Post-lockdown (1 March–31 March) periods in 2019 and 2020, along with the associated premature deaths due to short-term exposure to PM<sub>2.5</sub> (c) and O<sub>3</sub> (d). Figure S3. Cumulative distribution of population living under different ambient PM<sub>2.5</sub> concentrations in Shandong province from 2014 to 2020. Figure S4. Temporal variations in premature mortality due to long-term exposure to PM<sub>2.5</sub> (a) and O<sub>3</sub> (b) in Shandong province at the city level from 2014 to 2020. Figure S5. The set of AF change curves for each health endpoint at corresponding PM<sub>2.5</sub> concentrations. Figure S6. Premature mortality associated with short-term exposure to PM<sub>2.5</sub> in different pollution levels in PCEEC, WERB, and SPBEZ from 2014 to 2020. Figure S7. Premature mortality due to short-term exposure to PM<sub>2.5</sub> in different PM<sub>2.5</sub> pollution levels by city from 2014 to 2020. Figure S8. Percentage and number of the population aged 65+ in Shandong province in the future. Table S1. Fitting parameters and thresholds used in the exposure–response functions. Table S2. Baseline mortality data of specific diseases from 2014 to 2020. Table S3. Annual average concentrations of PM<sub>2.5</sub> and O<sub>3</sub> in Shandong province from 2025 to 2060. Table S4. The introduction and implementation of policies related to clean air actions in Shandong province. Table S5. Top 30 counties with the highest premature mortality rates due to long-term PM<sub>2.5</sub> exposure from 2014 to 2020. Table S6. Premature mortality associated with long- and short-term exposures to PM<sub>2.5</sub> (95% confidence interval (in thousand)) in Shandong province from 2014 to 2020. Table S7. Top 30 counties with the highest premature mortality rates due to long-term O<sub>3</sub> exposure from 2014 to 2020. Table S8. Premature mortality associated with short-term exposure to O<sub>3</sub> (95% confidence interval) in 16 cities from Shandong province from 2014 to 2020. Table S9. Driving force changes in premature mortality for each health endpoint associated with long-term exposure to PM<sub>2.5</sub> and O<sub>3</sub>, 2014–2020 (unit: thousand).

**Author Contributions:** Conceptualization, C.Z. (Chuanyong Zhu) and C.Z. (Changtong Zhu); data curation, M.Q., Y.G. and R.L.; funding acquisition, C.Z. (Chuanyong Zhu) and L.S.; methodology, C.Z. (Changtong Zhu) and C.Z. (Chuanyong Zhu); project administration, C.Z. (Chuanyong Zhu); resources, C.Z. (Chuanyong Zhu) and C.Z. (Changtong Zhu); software, N.Y., C.W. and B.W.; supervision, C.Z. (Chuanyong Zhu) and C.Z. (Changtong Zhu); validation, C.X.; visualization, C.Z. (Changtong Zhu); writing—original draft, C.Z. (Changtong Zhu); writing—review and editing, L.L., G.Y., C.Z. (Chuanyong Zhu) and C.Z. (Changtong Zhu). All authors have read and agreed to the published version of the manuscript.

**Funding:** This work is jointly funded by the National Natural Science Foundation of China (21707075, 42105104), the Basic Research Program for Integration Pilot Project of Science, Education and Industry of Qilu University of Technology (Shandong Academy of Science) (2023PY005, 2023PY041, and 2023PX096), the Bidding (Major) Teaching Reform Project from Qilu University of Technology (Shandong Academy of Science) (Z202201), the Shandong Provincial Natural Science Foundation (ZR2020QD060), the Qilu University of Technology Talent Scientific Research Project (2023RCKY107), and the Major Innovation Projects of Science, Education and Industry Integration of Qilu University of Technology (Shandong Academy of Science) (2022JBZ02-05).

**Institutional Review Board Statement:** Not applicable.

**Informed Consent Statement:** Not applicable.

**Data Availability Statement:** The concentration data for PM<sub>2.5</sub> and O<sub>3</sub> are available at <http://tapdata.org.cn> (accessed on 20 September 2023). The population data are available at <https://landscan.ornl.gov/> (accessed on 20 September 2023). Other data presented in this study are available in the supplementary material to this article.

**Acknowledgments:** We would like to thank the students involved in this work.

**Conflicts of Interest:** The authors declare that they have no known competing financial interest or personal relationships that could have appeared to influence the work reported in this paper.

## References

1. Murray, C.J.L.; Aravkin, A.Y.; Zheng, P.; Abbafati, C.; Abbas, K.M.; Abbasi-Kangevari, M.; Abd-Allah, F.; Abdelalim, A.; Abdollahi, M.; Abdollahpour, I.; et al. Global burden of 87 risk factors in 204 countries and territories, 1990–2019: A systematic analysis for the Global Burden of Disease Study 2019. *Lancet* **2020**, *396*, 1223–1249. [[CrossRef](#)] [[PubMed](#)]
2. Brauer, M.; Casadei, B.; Harrington, R.A.; Kovacs, R.; Sliwa, K.; Group, W.H.F.A.P.E. Taking a Stand Against Air Pollution-The Impact on Cardiovascular Disease: A Joint Opinion from the World Heart Federation, American College of Cardiology, American Heart Association, and the European Society of Cardiology. *Circulation* **2021**, *143*, e800–e804. [[CrossRef](#)] [[PubMed](#)]
3. Burnett, R.; Chen, H.; Szyszkwicz, M.; Fann, N.; Hubbell, B.; Pope, C.A., 3rd; Apte, J.S.; Brauer, M.; Cohen, A.; Weichenthal, S.; et al. Global estimates of mortality associated with long-term exposure to outdoor fine particulate matter. *Proc. Natl. Acad. Sci. USA* **2018**, *115*, 9592–9597. [[CrossRef](#)] [[PubMed](#)]
4. Yao, M.; Wu, G.; Zhao, X.; Zhang, J. Estimating health burden and economic loss attributable to short-term exposure to multiple air pollutants in China. *Environ. Res.* **2020**, *183*, 109184. [[CrossRef](#)]
5. Geng, G.; Zheng, Y.; Zhang, Q.; Xue, T.; Zhao, H.; Tong, D.; Zheng, B.; Li, M.; Liu, F.; Hong, C.; et al. Drivers of PM<sub>2.5</sub> air pollution deaths in China 2002–2017. *Nat. Geosci.* **2021**, *14*, 645–650. [[CrossRef](#)]
6. Chen, Y.; Guo, F.; Wang, J.; Cai, W.; Wang, C.; Wang, K. Provincial and gridded population projection for China under shared socioeconomic pathways from 2010 to 2100. *Sci. Data* **2020**, *7*, 83. [[CrossRef](#)]
7. Li, K.; Jacob, D.J.; Liao, H.; Shen, L.; Zhang, Q.; Bates, K.H. Anthropogenic drivers of 2013–2017 trends in summer surface ozone in China. *Proc. Natl. Acad. Sci. USA* **2019**, *116*, 422–427. [[CrossRef](#)]
8. Lian, L.; Chen, S.; Ma, J.; Li, T.; Yang, Y.; Huang, T.; Wang, Y.; Li, J. Population Aging Driven Slowdown in the Reduction of Economic Cost-Attributed to PM<sub>2.5</sub> Pollution after 2013 in China. *Environ. Sci. Technol.* **2022**, *57*, 1237–1245. [[CrossRef](#)]
9. Guan, Y.; Kang, L.; Wang, Y.; Zhang, N.-N.; Ju, M.-T. Health loss attributed to PM<sub>2.5</sub> pollution in China’s cities: Economic impact, annual change and reduction potential. *J. Clean. Prod.* **2019**, *217*, 284–294. [[CrossRef](#)]
10. Song, C.B.; He, J.J.; Wu, L.; Jin, T.S.; Chen, X.; Li, R.P.; Ren, P.P.; Zhang, L.; Mao, H.J. Health burden attributable to ambient PM<sub>2.5</sub> in China. *Environ. Pollut.* **2017**, *223*, 575–586. [[CrossRef](#)]
11. Zou, B.; You, J.; Lin, Y.; Duan, X.; Zhao, X.; Fang, X.; Campen, M.J.; Li, S. Air pollution intervention and life-saving effect in China. *Environ. Int.* **2019**, *125*, 529–541. [[CrossRef](#)]
12. Yin, S. Decadal changes in PM<sub>2.5</sub>-related health impacts in China from 1990 to 2019 and implications for current and future emission controls. *Sci. Total Environ.* **2022**, *834*, 155334. [[CrossRef](#)]
13. Guan, Y.; Xiao, Y.; Rong, B.; Zhang, N.; Chu, C. Long-term health impacts attributable to PM<sub>2.5</sub> and ozone pollution in China’s most polluted region during 2015–2020. *J. Clean. Prod.* **2021**, *321*, 128970. [[CrossRef](#)]
14. Wang, Y.; Hu, J.; Zhu, J.; Li, J.; Qin, M.; Liao, H.; Chen, K.; Wang, M. Health Burden and economic impacts attributed to PM<sub>2.5</sub> and O<sub>3</sub> in China from 2010 to 2050 under different representative concentration pathway scenarios. *Resour. Conserv. Recycl.* **2021**, *173*, 105731. [[CrossRef](#)]
15. Li, X.; Zhao, H.Y.; Xue, T.; Geng, G.N.; Zheng, Y.X.; Li, M.; Zheng, B.; Li, H.Y.; Zhang, Q. Consumption-based PM<sub>2.5</sub>-related premature mortality in the Beijing-Tianjin-Hebei region. *Sci. Total Environ.* **2021**, *800*, 8. [[CrossRef](#)] [[PubMed](#)]
16. Lin, H.; Liu, T.; Xiao, J.; Zeng, W.; Li, X.; Guo, L.; Xu, Y.; Zhang, Y.; Vaughn, M.G.; Nelson, E.J.; et al. Quantifying short-term and long-term health benefits of attaining ambient fine particulate pollution standards in Guangzhou, China. *Atmos. Environ.* **2016**, *137*, 38–44. [[CrossRef](#)]
17. Xiao, Q.; Geng, G.; Xue, T.; Liu, S.; Cai, C.; He, K.; Zhang, Q. Tracking PM<sub>2.5</sub> and O<sub>3</sub> Pollution and the Related Health Burden in China 2013–2020. *Environ. Sci. Technol.* **2021**, *56*, 6922–6932. [[CrossRef](#)] [[PubMed](#)]
18. Liu, J.; Yin, H.; Tang, X.; Zhu, T.; Zhang, Q.; Liu, Z.; Tang, X.; Yi, H. Transition in air pollution, disease burden and health cost in China: A comparative study of long-term and short-term exposure. *Environ. Pollut.* **2021**, *277*, 116770. [[CrossRef](#)]
19. Shan, Y.; Huang, Q.; Guan, D.; Hubacek, K. China CO<sub>2</sub> emission accounts 2016–2017. *Sci. Data* **2020**, *7*, 54. [[CrossRef](#)]
20. Yang, H.; Lu, Z.N.; Shi, X.P.; Muhammad, S.; Cao, Y. How well has economic strategy changed CO<sub>2</sub> emissions? Evidence from China’s largest emission province. *Sci. Total Environ.* **2021**, *774*, 14. [[CrossRef](#)]
21. Rauner, S.; Hilaire, J.; Klein, D.; Strefler, J.; Luderer, G. Air quality co-benefits of ratcheting up the NDCs. *Clim. Chang.* **2020**, *163*, 1481–1500. [[CrossRef](#)]
22. Tong, D.; Geng, G.N.; Jiang, K.J.; Cheng, J.; Zheng, Y.X.; Hong, C.P.; Yan, L.; Zhang, Y.X.; Chen, X.T.; Bo, Y.; et al. Energy and emission pathways towards PM<sub>2.5</sub> air quality attainment in the Beijing-Tianjin-Hebei region by 2030. *Sci. Total Environ.* **2019**, *692*, 361–370. [[CrossRef](#)] [[PubMed](#)]
23. Zhou, M.; Wang, H.; Zhu, J.; Chen, W.; Wang, L.; Liu, S.; Li, Y.; Wang, L.; Liu, Y.; Yin, P.; et al. Cause-specific mortality for 240 causes in China during 1990–2013: A systematic subnational analysis for the Global Burden of Disease Study 2013. *Lancet* **2016**, *387*, 251–272. [[CrossRef](#)] [[PubMed](#)]

24. Burnett, R.T.; Pope, C.A., 3rd; Ezzati, M.; Olives, C.; Lim, S.S.; Mehta, S.; Shin, H.H.; Singh, G.; Hubbell, B.; Brauer, M.; et al. An integrated risk function for estimating the global burden of disease attributable to ambient fine particulate matter exposure. *Environ. Health Perspect.* **2014**, *122*, 397–403. [[CrossRef](#)]
25. Jiang, X.; Zhang, Q.; Zhao, H.; Geng, G.; Peng, L.; Guan, D.; Kan, H.; Huo, H.; Lin, J.; Brauer, M.; et al. Revealing the hidden health costs embodied in Chinese exports. *Environ. Sci. Technol.* **2015**, *49*, 4381–4388. [[CrossRef](#)]
26. Jerrett, M.; Burnett, R.T.; Pope, C.A.; Ito, K.; Thurston, G.; Krewski, D.; Shi, Y.L.; Calle, E.; Thun, M. Long-Term Ozone Exposure and Mortality. *N. Engl. J. Med.* **2009**, *360*, 1085–1095. [[CrossRef](#)]
27. Lelieveld, J.; Barlas, C.; Giannadaki, D.; Pozzer, A. Model calculated global, regional and megacity premature mortality due to air pollution. *Atmos. Chem. Phys.* **2013**, *13*, 7023–7037. [[CrossRef](#)]
28. Lu, F.; Xu, D.; Cheng, Y.; Dong, S.; Guo, C.; Jiang, X.; Zheng, X. Systematic review and meta-analysis of the adverse health effects of ambient PM<sub>2.5</sub> and PM<sub>10</sub> pollution in the Chinese population. *Environ. Res.* **2015**, *136*, 196–204. [[CrossRef](#)]
29. Madaniyazi, L.; Nagashima, T.; Guo, Y.; Pan, X.; Tong, S. Projecting ozone-related mortality in East China. *Environ. Int.* **2016**, *92–93*, 165–172. [[CrossRef](#)]
30. Yin, P.; Chen, R.; Wang, L.; Meng, X.; Liu, C.; Niu, Y.; Lin, Z.; Liu, Y.; Liu, J.; Qi, J.; et al. Ambient Ozone Pollution and Daily Mortality: A Nationwide Study in 272 Chinese Cities. *Environ. Health Perspect.* **2017**, *125*, 117006. [[CrossRef](#)] [[PubMed](#)]
31. Atkinson, R.W.; Butland, B.K.; Dimitroulopoulou, C.; Heal, M.R.; Stedman, J.R.; Carslaw, N.; Jarvis, D.; Heaviside, C.; Vardoulakis, S.; Walton, H.; et al. Long-term exposure to ambient ozone and mortality: A quantitative systematic review and meta-analysis of evidence from cohort studies. *BMJ Open* **2016**, *6*, e009493. [[CrossRef](#)] [[PubMed](#)]
32. Feng, Z.; De Marco, A.; Anav, A.; Gualtieri, M.; Sicard, P.; Tian, H.; Fornasier, F.; Tao, F.; Guo, A.; Paoletti, E. Economic losses due to ozone impacts on human health, forest productivity and crop yield across China. *Environ. Int.* **2019**, *131*, 104966. [[CrossRef](#)] [[PubMed](#)]
33. Liu, H.; Liu, S.; Xue, B.; Lv, Z.; Meng, Z.; Yang, X.; Xue, T.; Yu, Q.; He, K. Ground-level ozone pollution and its health impacts in China. *Atmos. Environ.* **2018**, *173*, 223–230. [[CrossRef](#)]
34. Wang, F.Y.; Qiu, X.H.; Cao, J.Y.; Peng, L.; Zhang, N.N.; Yan, Y.L.; Li, R.M. Policy-driven changes in the health risk of PM<sub>2.5</sub> and O<sub>3</sub> exposure in China during 2013–2018. *Sci. Total Environ.* **2021**, *757*, 9. [[CrossRef](#)]
35. Cohen, A.J.; Brauer, M.; Burnett, R.; Anderson, H.R.; Frostad, J.; Estep, K.; Balakrishnan, K.; Brunekreef, B.; Dandona, L.; Dandona, R.; et al. Estimates and 25-year trends of the global burden of disease attributable to ambient air pollution: An analysis of data from the Global Burden of Diseases Study 2015. *Lancet* **2017**, *389*, 1907–1918. [[CrossRef](#)]
36. Yue, H.; He, C.; Huang, Q.; Yin, D.; Bryan, B.A. Stronger policy required to substantially reduce deaths from PM<sub>2.5</sub> pollution in China. *Nat. Commun.* **2020**, *11*, 1462. [[CrossRef](#)]
37. Jin, X.; Cai, X.; Yu, M.; Wang, X.; Song, Y.; Wang, X.; Zhang, H.; Zhu, T. Regional PM<sub>2.5</sub> pollution confined by atmospheric internal boundaries in the North China Plain: Analysis based on surface observations. *Sci. Total Environ.* **2022**, *841*, 156728. [[CrossRef](#)]
38. Yao, Y.; He, C.; Li, S.; Ma, W.; Li, S.; Yu, Q.; Mi, N.; Yu, J.; Wang, W.; Yin, L.; et al. Properties of particulate matter and gaseous pollutants in Shandong, China: Daily fluctuation, influencing factors, and spatiotemporal distribution. *Sci. Total Environ.* **2019**, *660*, 384–394. [[CrossRef](#)]
39. Zhao, N.; Wang, G.; Li, G.; Lang, J. Trends in Air Pollutant Concentrations and the Impact of Meteorology in Shandong Province, Coastal China, during 2013–2019. *Aerosol Air Qual. Res.* **2021**, *21*, 200545. [[CrossRef](#)]
40. Zhang, J.; Zhou, X.; Wang, Z.; Yang, L.; Wang, J.; Wang, W. Trace elements in PM<sub>2.5</sub> in Shandong Province: Source identification and health risk assessment. *Sci. Total Environ.* **2018**, *621*, 558–577. [[CrossRef](#)]
41. Zhou, Y.; Zi, T.; Lang, J.L.; Huang, D.W.; Wei, P.; Chen, D.S.; Cheng, S.Y. Impact of rural residential coal combustion on air pollution in Shandong, China. *Chemosphere* **2020**, *260*, 9. [[CrossRef](#)] [[PubMed](#)]
42. National Bureau of Statistics of China (NBSC). *China Energy Statistical Yearbook*; China Statistics Press: Beijing, China, 2021. (In Chinese)
43. Wu, R.; Xie, S. Spatial Distribution of Ozone Formation in China Derived from Emissions of Speciated Volatile Organic Compounds. *Environ. Sci. Technol.* **2017**, *51*, 2574–2583. [[CrossRef](#)] [[PubMed](#)]
44. Dang, R.; Liao, H.; Fu, Y. Quantifying the anthropogenic and meteorological influences on summertime surface ozone in China over 2012–2017. *Sci. Total Environ.* **2021**, *754*, 142394. [[CrossRef](#)] [[PubMed](#)]
45. Ou, J.; Yuan, Z.; Zheng, J.; Huang, Z.; Shao, M.; Li, Z.; Huang, X.; Guo, H.; Louie, P.K. Ambient Ozone Control in a Photochemically Active Region: Short-Term Despiking or Long-Term Attainment? *Environ. Sci. Technol.* **2016**, *50*, 5720–5728. [[CrossRef](#)] [[PubMed](#)]
46. Bei, N.; Zhao, L.; Wu, J.; Li, X.; Feng, T.; Li, G. Impacts of sea-land and mountain-valley circulations on the air pollution in Beijing-Tianjin-Hebei (BTH): A case study. *Environ. Pollut.* **2018**, *234*, 429–438. [[CrossRef](#)] [[PubMed](#)]
47. Li, K.; Jacob, D.J.; Liao, H.; Zhu, J.; Shah, V.; Shen, L.; Bates, K.H.; Zhang, Q.; Zhai, S. A two-pollutant strategy for improving ozone and particulate air quality in China. *Nat. Geosci.* **2019**, *12*, 906–910. [[CrossRef](#)]
48. Wang, Z.; Yan, J.; Zhang, P.; Li, Z.; Guo, C.; Wu, K.; Li, X.; Zhu, X.; Sun, Z.; Wei, Y. Chemical characterization, source apportionment, and health risk assessment of PM<sub>2.5</sub> in a typical industrial region in North China. *Environ. Sci. Pollut. Res. Int.* **2022**, *29*, 71696–71708. [[CrossRef](#)]
49. Zhang, G.; Ding, C.; Jiang, X.; Pan, G.; Wei, X.; Sun, Y. Chemical Compositions and Sources Contribution of Atmospheric Particles at a Typical Steel Industrial Urban Site. *Sci. Rep.* **2020**, *10*, 7654. [[CrossRef](#)]

50. Zhao, X.; Wang, J.; Xu, B.; Zhao, R.; Zhao, G.; Wang, J.; Ma, Y.; Liang, H.; Li, X.; Yang, W. Causes of PM<sub>2.5</sub> pollution in an air pollution transport channel city of northern China. *Environ. Sci. Pollut. Res. Int.* **2022**, *29*, 23994–24009. [[CrossRef](#)]
51. Cheng, M.; Tang, G.; Lv, B.; Li, X.; Wu, X.; Wang, Y.; Wang, Y. Source apportionment of PM<sub>2.5</sub> and visibility in Jinan, China. *J. Environ. Sci.* **2021**, *102*, 207–215. [[CrossRef](#)]
52. Jiang, P.; Chen, X.; Li, Q.; Mo, H.; Li, L. High-resolution emission inventory of gaseous and particulate pollutants in Shandong Province, eastern China. *J. Clean. Prod.* **2020**, *259*, 120806. [[CrossRef](#)]
53. Zhou, M.; Jiang, W.; Gao, W.; Gao, X.; Ma, M.; Ma, X. Anthropogenic emission inventory of multiple air pollutants and their spatiotemporal variations in 2017 for the Shandong Province, China. *Environ. Pollut.* **2021**, *288*, 117666. [[CrossRef](#)] [[PubMed](#)]
54. Zhu, S.; Poetscher, J.; Shen, J.; Wang, S.; Wang, P.; Zhang, H. Comprehensive Insights Into O<sub>3</sub> Changes during the COVID-19 from O<sub>3</sub> Formation Regime and Atmospheric Oxidation Capacity. *Geophys. Res. Lett.* **2021**, *48*, e2021GL093668. [[CrossRef](#)] [[PubMed](#)]
55. Xiao, Q.; Zheng, Y.; Geng, G.; Chen, C.; Huang, X.; Che, H.; Zhang, X.; He, K.; Zhang, Q. Separating emission and meteorological contributions to long-term PM<sub>2.5</sub> trends over eastern China during 2000–2018. *Atmos. Chem. Phys.* **2021**, *21*, 9475–9496. [[CrossRef](#)]
56. Gong, S.; Liu, H.; Zhang, B.; He, J.; Zhang, H.; Wang, Y.; Wang, S.; Zhang, L.; Wang, J. Assessment of meteorology vs. control measures in the China fine particulate matter trend from 2013 to 2019 by an environmental meteorology index. *Atmos. Chem. Phys.* **2021**, *21*, 2999–3013. [[CrossRef](#)]
57. Wei, Y.; Wang, Z.; Wang, H.; Li, Y.; Jiang, Z. Predicting population age structures of China, India, and Vietnam by 2030 based on compositional data. *PLoS ONE* **2019**, *14*, e0212772. [[CrossRef](#)]
58. Wang, F.; Liang, Q.; Sun, M.; Ma, Y.; Lin, L.; Li, T.; Duan, J.; Sun, Z. The relationship between exposure to PM<sub>2.5</sub> and heart rate variability in older adults: A systematic review and meta-analysis. *Chemosphere* **2020**, *261*, 127635. [[CrossRef](#)]
59. Yin, H.; Brauer, M.; Zhang, J.; Cai, W.; Navrud, S.; Burnett, R.; Howard, C.; Deng, Z.; Kammen, D.M.; Schellnhuber, H.J.; et al. Population ageing and deaths attributable to ambient PM<sub>2.5</sub> pollution: A global analysis of economic cost. *Lancet Planet Health* **2021**, *5*, e356–e367. [[CrossRef](#)]
60. Zheng, B.; Zhang, Q.; Geng, G.; Chen, C.; Shi, Q.; Cui, M.; Lei, Y.; He, K. Changes in China’s anthropogenic emissions and air quality during the COVID-19 pandemic in 2020. *Earth Syst. Sci. Data* **2021**, *13*, 2895–2907. [[CrossRef](#)]
61. Ginter, E.; Simko, V. Women live longer than men. *Bratisl. Lek. Listy* **2013**, *114*, 45–49. [[CrossRef](#)]
62. Shi, X.; Zheng, Y.; Lei, Y.; Xue, W.; Yan, G.; Liu, X.; Cai, B.; Tong, D.; Wang, J. Air quality benefits of achieving carbon neutrality in China. *Sci. Total Environ.* **2021**, *795*, 148784. [[CrossRef](#)] [[PubMed](#)]
63. Wang, J.; Yang, Y.; Zhang, Y.; Niu, T.; Jiang, X.; Wang, Y.; Che, H. Influence of meteorological conditions on explosive increase in O<sub>3</sub> concentration in troposphere. *Sci. Total Environ.* **2019**, *652*, 1228–1241. [[CrossRef](#)] [[PubMed](#)]
64. Ding, D.; Xing, J.; Wang, S.; Dong, Z.; Zhang, F.; Liu, S.; Hao, J. Optimization of a NO<sub>x</sub> and VOC Cooperative Control Strategy Based on Clean Air Benefits. *Environ. Sci. Technol.* **2021**, *56*, 739–749. [[CrossRef](#)] [[PubMed](#)]
65. Simayi, M.; Shi, Y.; Xi, Z.; Ren, J.; Hini, G.; Xie, S. Emission trends of industrial VOCs in China since the clean air action and future reduction perspectives. *Sci. Total Environ.* **2022**, *826*, 153994. [[CrossRef](#)] [[PubMed](#)]

**Disclaimer/Publisher’s Note:** The statements, opinions and data contained in all publications are solely those of the individual author(s) and contributor(s) and not of MDPI and/or the editor(s). MDPI and/or the editor(s) disclaim responsibility for any injury to people or property resulting from any ideas, methods, instructions or products referred to in the content.